Black Body Fragmentation of Cationic Ammonia Clusters

Brigitte S. Fox, Martin K. Beyer, and Vladimir E. Bondybey*

Institut für Physikalische und Theoretische Chemie, Technische Universität München, Lichtenbergstrasse 4, 85747 Garching, Germany

Received: January 4, 2001; In Final Form: April 2, 2001

We have carried out a systematic study of the blackbody radiation induced fragmentation of size-selected ionic ammonia clusters and compared it with that of the corresponding hydrates. Specifically, the Ag^+ and H^+ cation clusters were studied, with the fragmentation rate constants of the ions solvated with ammonia being found to exhibit the same overall linear dependence on the number of ligands *n*, which was previously observed for the corresponding hydrates as well as for a number of other hydrated ions. To facilitate the interpretation of the experimental observations, we have carried out DFT calculations of the cluster structures and of their harmonic frequencies and intensities. The observed fragmentation rate constants exhibit a satisfactory qualitative agreement with the computed rates of energy absorption from the blackbody infrared radiation background.

Introduction

Molecular clusters bridge the gap between discrete gas-phase molecules and bulk condensed phases, and their properties are therefore of considerable interest.[1,2] In recent years, Fourier transform ion cyclotron resonance mass spectrometry (FT-ICR) has become a very productive technique with which a large variety of ionic clusters has been investigated. These FT-ICR studies have revealed that while relatively weakly bound clusters with ligands such as argon atoms or molecular nitrogen can be trapped in the ICR cell for many seconds or even minutes, hydrogen bonded cluster ions, despite the much stronger bonds, continuously fragment on a millisecond time scale due to the absorption of infrared blackbody radiation from the apparatus walls.[3−9]

Water is by far the most common solvent, important not only in industry and technology but also in the environment around us. Water molecules are highly polar, they interact strongly with the dissolved solutes, in particular ions, and have a significant effect upon their properties and chemical reactions. The blackbody fragmentation provides a unique tool for gently removing water ligands from an ionic cluster one by one, and allowing observation of the effects due to loss of the stabilizing solvent from the system under investigation. Individual solvent molecules evaporate in the essentially collision free, high vacuum environment from the hydrated anionic or cationic clusters due to infrared absorption by the water ligands. The rate of the overall energy input, and therefore of the solvent evaporation, is roughly proportional to the number of ligand molecules *n*.[9−13] We have taken advantage of this effect to explore in a microscopic, molecular detail, a number of different aqueous reactions taking place in the hydrated clusters or "nanodroplets".[14−18] The reason why the hydrated clusters fragment, but ions ligated by for instance rare gases, CO or nitrogen do not is that unlike the relatively nonpolar latter ligands, the cluster modes of the hydrogen bonded water network overlap efficiently the room temperature Planck blackbody emission function.

Water is, however, not unique in this behavior, and one might expect other polar and strongly absorbing systems to behave in a similar way. Another important polar solvent which like water efficiently solvates ions and stabilizes ionic species is ammonia. More importantly, similar to water it has the ability to form strong hydrogen bonds, which in general greatly enhance the transition dipole of infrared transitions. Furthermore, solvating the ions by ammonia also results, similar to hydrated clusters, in the appearance of numerous low frequency intermolecular "translational" or "rotational" modes, which ideally overlap the 300 K blackbody background radiation distribution. Besides similarities, there are also some important differences between the two solvents. For instance, it is also well-known that neutral NH_3 forms considerably weaker hydrogen bonds than water as evidenced e.g. by the lower binding energies of the dimers (ammonia, <11.72 kJ/mol;[19] water dimer, 22.6 ± 2.9 kJ/mol[20−22]).

Even more importantly, a water molecule can form two donor and two acceptor hydrogen bonds, as evidenced by the tetracoordination which is characteristic both for solid ice and for liquid water and aqueous solutions. In contrast with that, NH_3 could in principle form three donor bonds, but possesses only a single lone pair to form acceptor bonds, making the formation of extended hydrogen bonded networks more difficult. These two differences result in the considerably higher vapor pressure and lower boiling point of liquid NH_3 as compared with water, despite the comparable molecular weights of the two solvents. Because of the fact that ammonia is unable to form more than one acceptor hydrogen bond, one might expect in cationic clusters the single nitrogen lone pair of the first solvation shell ammonia ligands to coordinate the central core ion, making the formation of rings less probable and favoring branched structures, and this in turn makes extensive networks less stable. This view is supported by recent ab initio calculations of $H^+(NH_3)_n$ ($n = 1-8$),[23] which report optimized geometries resembling NH_4+ ammonium cation core, bound by "donor" hydrogen bonds to up to four ammonia molecules, with the sixth to eighth ammonia ligands appearing in the second solvation shell. Somewhat different results were recently reported by

* To whom correspondence should be addressed. Fax: +49 89 289 1 34 16. E-mail: bondybey@ch.tum.de.

10.1021/jp0100452 CCC: $20.00
Published on Web 06/08/2001

Bérces et al., who found in the geometries of the $[Cu(NH_3)_n]^{2+}$, $n = 3-8$ ions, optimized by static DFT and ab initio molecular dynamics calculations also stationary points with ammonia in bridging position forming two acceptor bonds.[24] Since, however, no vibrational frequencies were apparently calculated, these might represent transition states.

The investigation of the blackbody radiation induced fragmentation provides useful information about cluster stability, and may also yield some insight into their structure. We report here the results of a first systematic study of the blackbody fragmentation of ionic ammonia clusters, and of ions solvated by ammonia, and their comparison with the analogous hydrated systems. Specifically we concentrate here on solvated Ag^+, but examine also $H^+(NH_3)_n$ species, in view of the detailed previous studies of the hydrated $H^+(H_2O)_n$, $n = 5-65$, cluster ions.[9,10]

Experimental Details

The experiments were performed on a modified Spectrospin CMS47X mass spectrometer described in detail elsewhere.[25,26] The cluster ions were generated in a pulsed supersonic expansion source using 10 bar of helium carrier gas seeded with about 30 mbar of either water vapor or ammonia. Metal cations were produced by laser vaporization of a solid silver disk (Chempur, 99.995%+), and the plasma produced by the laser was then entrained in a pulse of the carrier gas. It was cooled by flowing through a confining channel with the clustering and solvation of the ions taking place in the subsequent supersonic expansion into high vacuum. The size and nature of the ions formed was controlled by changing the source parameters, especially laser power and pulse timing. While at lower laser powers the source can be optimized to generate predominantly solvated metal—in the present case, silver—cations, by increasing the laser pulse energy and adjusting the delay between the piezoelectric valve trigger and the Q-switch of the Nd:YAG laser, conditions can be found where almost exclusively solvated proton clusters are produced. Laser vaporization thus provides an even more convenient and efficient source of protonated clusters than the discharge source previously used in our laboratory.[9,10] In either case, the cluster ions produced in the source are transferred through several stages of differential pumping into the high-field region of the superconducting magnet and stored inside the ICR cell at a background pressure of about 6×10^{-10} mbar. After allowing varying delays for the clusters to fragment or react, the ions remaining in the cell were detected, and the fragmentation products identified by their mass spectra. During all experiments, the vacuum chamber enclosing the ICR cell was cooled by a flow of water through the cooling jacket, resulting in a constant temperature of the apparatus walls of $T = 291 \pm 5$ K.

Computational Details

Computations were carried out on a Pentium III based Linux system using the Gaussian98[27] program package, employing the three-parameter hybrid Hartree—Fock/Density functional (B3LYP) method described by Becke[28-30] with the Lee—Yang—Parr correlation functional[31] as incorporated in Gaussian98. The 6-31G(d,p) basis set on all atoms was used for the geometry optimizations and frequency calculations, and also zero-point corrections were taken from this level of theory. In most of our optimizations, we have started from the structures found by Park[23b] for our $H^+(NH_3)_n$, $n = 1-5$, computations. For $H^+(H_2O)_n$, $n = 4$ or 5, only the solvated H_3O^+ structures, known to be global minima,[32-34] were optimized. Single-point energy calculations were performed employing the larger 6-311++G-(3df,3pd) basis set on all atoms. The power absorbed by the cluster modes from 298 K blackbody radiation was calculated from the overlap between the 300 K Planck distribution function and the cluster infrared spectrum and intensities $I(\nu)$ taken from the DFT calculations. The power P in kW/mol absorbed at a frequency ν is obtained from the following equation,[35] where ν is in cm^{-1} and I is in km/mol:

$$P(\nu,I,T) = \frac{8\pi hc^2\nu^3 I \times 10^6}{\exp(100\, ch\nu/kT) - 1} \qquad (1)$$

No scaling factor for the computed frequencies was used, since the errors resulting from uncertainties in the computed intensities are probably considerably larger than those due to the frequency errors.

With the knowledge of vibrational frequencies of the solvated ions, it is also possible to compute the average internal energies as a function of temperature, which are useful in understanding cluster stability and fragmentation. To estimate the internal energies we have assumed the clusters behave as ensembles of independent harmonic oscillators, and computed and summed the expectation values of the energies of each of these oscillators.

Results and Discussion

Formation of Protonated Cluster $H^+(NH_3)_n$ and $H^+(H_2O)_n$ in the Laser Vaporization Source. With increasing laser pulse energy, the solvated metal ion clusters $Ag^+(NH_3)_n$ and $Ag^+(H_2O)_n$ disappear, and $H^+(NH_3)_n$ and $H^+(H_2O)_n$ become the dominant species in the spectra. In fact, conditions are readily found where the protonated clusters are exclusively observed, while it is comparatively hard to completely eliminate protonated clusters from the solvated metal ion spectra. The explanation for this can be found in the literature. Barnett and Landman[38] review their own computational work[39] and experimental work by Ng et al.[40] and Tomoda and Kimura.[41] In the photoionization of the water dimer, the "oxonium" channel $(H_2O)_2 + h\nu \rightarrow H_3O^+ + OH + e^-$, is favored over the "water channel" $(H_2O)_2 + h\nu \rightarrow H_2O^+ + H_2O + e^-$ by 1.08 eV (calculated) or 1.13 eV (experimentally).[40,41] In our laser vaporization source, ionization of water may not only occur by direct absorption of multiple photons, but also, and more likely so, by collisions with highly excited atoms or ions from the metal plasma. Since the $H_3O^+ + OH$ products are thermochemically favored over $H_2O^+ + H_2O$, individual water cations H_2O^+ will react with other water molecules or clusters to form the protonated species.

Similar arguments apply to the ammonia clusters, with the large body of experimental work reviewed by Park.[23b] From tabulated thermochemistry data,[36] the reaction $NH_3^+ + NH_3 \rightarrow NH_4^+ + NH_2$ is calculated to be exothermic by -58.9 kJ/mol, which illustrates further that in the ion source and in the subsequent evaporative cooling of the clusters during the transfer into the ICR cell, any $(NH_3)_n^+$ species will be converted to $H^+(NH_3)_{n-1}$ by loss of an NH_2 amino radical.

Hydrated Cation Clusters: $Ag^+(H_2O)_n$ and $H^+(H_2O)_n$. Since comparison of cations solvated with ammonia with hydrated clusters is one of the major aims of this paper, we will first discuss briefly the aqueous clusters. As noted above, we have investigated the fragmentation of hydrated protons, $H^+(H_2O)_n$, previously in considerable detail.[9,10] A similar experiment for hydrated silver cations, $Ag^+(H_2O)_n$, is documented in Figure 1 which shows the initial $t = 0$ cluster distribution and its changes after various time delays. While at $t = 0$ (see Figure 1a) the distribution exhibits a maximum at $n = 18$ and extends from $n = 10-28$, the shift to smaller sizes at $t = 3$ and 10 s is

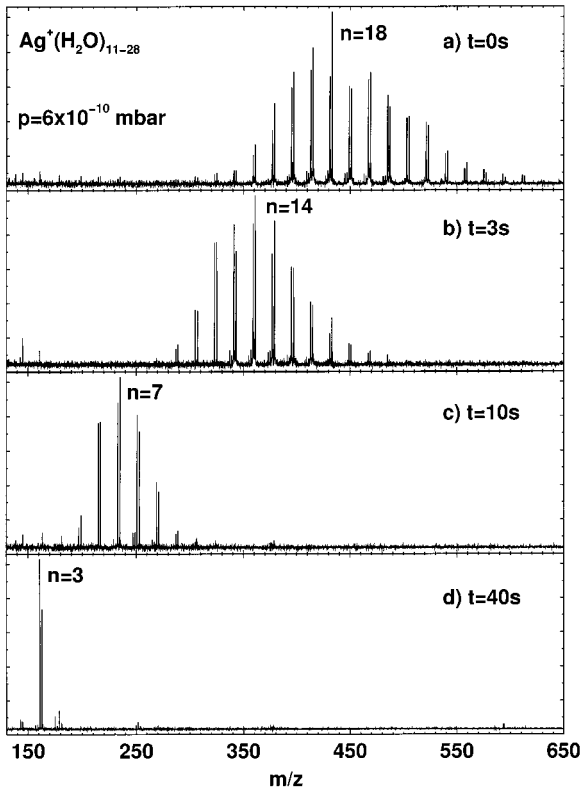

Figure 1. Mass spectra showing the fragmentation of $Ag^+(H_2O)_n$ clusters, $n = 10-28$, after variable reaction delays. At the pressure of about 6×10^{-10} mbar in the cell region, the fragmentation is induced by the IR background radiation. The labeled peaks in each panel denote the maximum of the distribution.

apparent in parts b and c, and after a reaction time of 40 s in Figure 1d, essentially only the final product $Ag^+(H_2O)_3$ can be seen. This can be compared with the hydrated proton experiments where the "final" product was $H^+(H_2O)_4$. As in our previous studies, one can take advantage of the ability of the FT-ICR technique to mass select a cluster of any desired size n in order to get a more detailed information about the fragmentation process. After the mass selection, the reaction delays can be varied, and the intensities of the reactant ion as well as of the products of its fragmentation recorded as a function of time, and the data fitted assuming first-order reaction kinetics.

Fragmentation rates of mass selected $Ag^+(H_2O)_n$, $n = 4-45$, obtained in this way are plotted against n in Figure 2a), where the solid circles give the experimental measurements, and the continuous line represents a linear least-squares fit of these data. From the diagram it is apparent that the rates increase approximately linearly with the number of ligands n. The data can be well fitted by an expression $k_n = k_f(n - n_0)$ where in the present case, $k_f = 0.18\ s^{-1}$, and $n_0 = 3.00$. This overall linear n dependence is in agreement with our earlier observations for hydrated protons, $H^+(H_2O)_n$ (see Figure 3a), where the analogous fitting procedure for $n = 5-65$ yielded constants $k_f = 0.20\ s^{-1}$ and $n_0 = 1.39$.[9,10] Comparable results, including similar slopes of the rate constant n dependence, were also found in our previous studies of numerous other hydrated ions, including the Mg^+ and Al^+ cations or I^- anions.[11-13]

Some of the constants obtained in this way for various solvated ions are summarized in Table 1. One can see that independent of the specific nature or charge of the central ion, the slope has for all the hydrated ions an almost identical value of $k_f = 0.18\ s^{-1}$. While small differences can be found in the table between the constants obtained for various central ions,

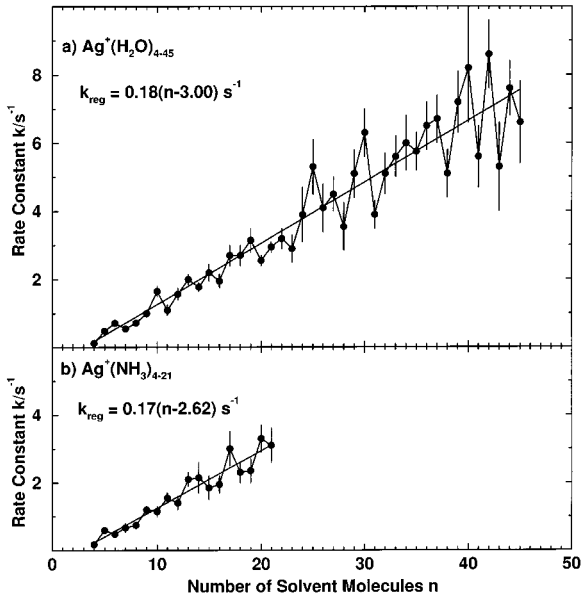

Figure 2. Unimolecular fragmentation rate constants for the blackbody radiation induced fragmentation of clusters as a function of the number of ligands n. The rate for each size selected cluster was obtained by fitting the initial signal decay, the solid line represents a linear fit to the expression $k_n = k_f(n - n_0)$ $[s^{-1}]$: (a) $Ag^+(H_2O)_n$, $n = 4-45$, $k_f = 0.18\ s^{-1}$, $n_0 = 3.00$. (b) $Ag^+(NH_3)_n$, $n = 4-21$, $k_f = 0.17\ s^{-1}$, $n_0 = 2.62$.

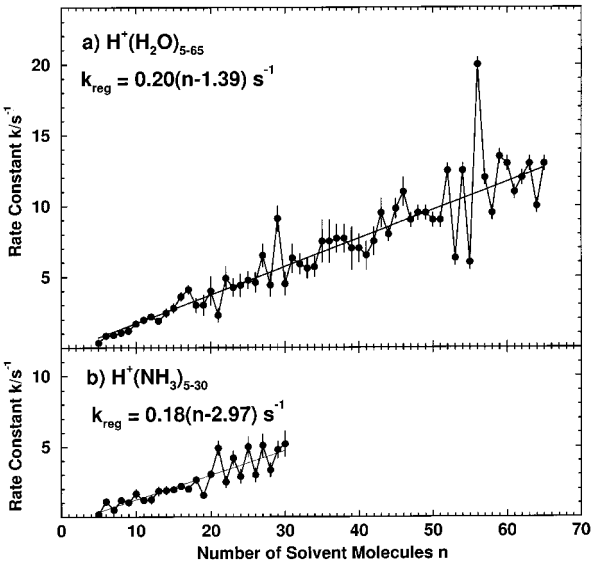

Figure 3. Unimolecular rate constants for the blackbody radiation induced fragmentation of (a) size-selected $H^+(H_2O)_n$ clusters, $n = 5-65$. Linear regression of these rate constants yields a straight line with $k_n = 0.20(n - 1.39)\ s^{-1}$. (b) $H^+(NH_3)_n$, $n = 5-30$. The data points can be fitted by the equation $k_n = 0.18(n - 2.97)\ s^{-1}$.

TABLE 1: Slopes k_f, Standard Errors of the Slopes and Intercepts n_0 Obtained by Fitting the Fragmentation Rate Constants to the Expression $k_n = k_f(n - n_0)$

cluster ions	slope k_f $[s^{-1}]$	standard error of slope $[s^{-1}]$	intercept n_0
$Ag^+(H_2O)_n$	0.18	0.01	3.00
$H^+(H_2O)_n$	0.20[a]	0.01	1.39
$Mg^+(H_2O)_n$	0.17[b]	0.02	2.35
$Al^+(H_2O)_n$	0.16[c]	0.02	1.63
$I^-(H_2O)_n$	0.17[d]	0.01	1.53
$Ag^+(NH_3)_n$	0.17	0.01	2.94
$H^+(NH_3)_n$	0.18	0.02	2.98

[a] Reference 10. [b] Reference 11. [c] Reference 12. [d] Reference 13.

one should not try to overinterpret them. Most of the differences are within the experimental error, and furthermore the exact values depend somewhat on the data field, that is on the range of cluster sizes *n* included in the fit, and these are different for different ions. Obviously, the specific nature and size of the central ion should have some effect upon its fragmentation and therefore on the magnitude of k_f, especially where the range of cluster sizes is relatively narrow. However, the similarity of the k_f values seen in Table 1 for the hydrates of quite different ions suggests that this effect of the central ion is relatively minor.

Comparison with Clusters Solvated by Ammonia: $Ag^+(NH_3)_n$ and $H^+(NH_3)_n$. We shall now turn to cations solvated by ammonia, which are the main topic of this paper. As already noted in the experimental part, ammonia clusters are formed in our source with almost equal ease as aqueous clusters, and we have investigated both solvated protons as well as solvated Ag^+ cations. Examination of such clusters solvated by ammonia reveals a very similar behavior to that found for the hydrated ions. Like the hydrates, also the ammonia clusters gradually fragment, and the initial cluster size distribution progressively shifts to smaller values of n. One finds again that not all of the ligands are lost, but even after very long delays "final" products are obtained, which do not seem to fragment further. For the clusters studied here, these are $Ag^+(NH_3)_3$ and $H^+(NH_3)_4$. Like their hydrated counterparts, the investigated ammonia clusters also show a linear dependence of the fragmentation rate on the number of ligand molecules as can be clearly seen in parts b of Figures 2 and 3. Linear fitting of the experimental data yields the equations $k_n = 0.17(n\text{-}2.62)$ s^{-1} for $Ag^+(NH_3)_n$ and $k_n = 0.18(n\text{-}2.97)$ s^{-1} for $H^+(NH_3)_n$, respectively, with the constants k_f and n_0 also included in Table 1. Somewhat surprisingly, one finds that also the slopes obtained by fitting the ammonia data seem to agree within the experimental error with those observed for the hydrated ions.

As explained previously for the hydrated ions, the linear dependence of the fragmentation rate can easily be understood. The temperature of the larger, fragmenting clusters, is determined by a competition between radiative heating and evaporative cooling,[9] and one can fairly easily show that they must be relatively cold compared with the ambient walls. For clusters around $n = 30-50$ one can estimate temperatures in the range of 100−150 K,[9] so that the energy loss due to "blackbody" emission of the clusters themselves can to a good approximation be neglected. Each time a cluster loses a ligand, an energy comparable to its "enthalpy of vaporization" is removed, and the cluster effective "temperature" sinks drastically. Because there are effectively no collisions, before another ligand can evaporate, the cluster has to absorb from the IR blackbody background at least enough energy to compensate for this loss, and for the temperature to approach again its original value. The energy is primarily absorbed by the hydrogen bonded ligand network, and therefore the overall rate of the energy absorption, as well as the rate of fragmentation, must be roughly proportional to the number of ligand molecules n. The physical meaning of the inverse of the constant, $1/k_f$, can thus approximately be seen as the time which would be needed by a single ligand molecule in the cluster to absorb from the blackbody background radiation an energy equivalent to the vaporization enthalpy of the ligand.

Obviously the energy needed to evaporate a ligand is not the same for all cluster sizes, but must itself be dependent on the value of *n*. In smaller clusters the ligands are closer to the central ion and feel its charge more strongly, and will therefore be more tightly bound than the "surface" ligands in larger clusters. Furthermore, often some specific "magic" cluster sizes exhibit higher stability than other nearby cluster sizes, perhaps due to an energetically particularly advantageous closed shell structure. It should also be realized that a ligand will not necessarily immediately "evaporate" as soon as the energetic threshold is reached. The rate of evaporation will depend on the energy excess above this threshold, and also this dependence itself will, based on statistical RRKM theories, be a function of the density of states, and thus of *n*, the size of the cluster. These secondary effects are, however, apparently not important enough to mask the basic, linear dependence of the fragmentation rates upon the cluster size *n*.

According to the above discussion, the constant k_f, that is the slope of the k_n rate against *n* plot is basically dependent on two factors, the ligand binding energy and the rate of energy absorption, where in turn, the latter factor should depend on the overlap integral between the ligand absorption spectrum and the Planck blackbody function at the ambient temperature. Obviously, the k_f constant should show linear dependence on the latter factor, but be inversely proportional to the former one, the energy needed to "evaporate" one ligand. In other words, the faster the rate of energy absorption, and the lower the ligand binding energy, the faster the cluster will fragment, and vice versa.

The binding energies of hydrated clusters and of clusters solvated with ammonia should, in general, be expected to be different. On one hand, the proton affinity of ammonia, 854.6 kJ/mol,[36] which will surely be important for the stability of the smallest protonated clusters, is considerably larger than that of water, 691 kJ/mol.[36] On the other hand, however, as already mentioned above, the neutral dimer of ammonia is considerably weaker bound than that of water. The most relevant properties one should probably use to compare the fragmentation behavior of the larger cluster ions should be the vaporization enthalpies of the two solvents, whose measured values at 298 K are 43.98 kJ/mol for H_2O and 19.86 kJ/mol for NH_3.[37] The larger experimental value found for water again reflects its ability to form two donor and two acceptor hydrogen bonds, which is ideally suited for the formation of extended ligand networks. Despite this factor of 2 difference in the vaporization enthalpies, one finds that the two slopes k_f for ammonia and water ligands are almost identical. One has to conclude that this is most likely fortuitous, and that the factor of 2 decrease in the binding of ammonia ligands must be almost exactly compensated by their less efficient absorption of the blackbody radiation.

Since we have computed both the vibrational frequencies and intensities of the vibrational transitions for several of the small solvated ions whose optimized geometries are shown in Figure 4, the overlap of their spectra with the Planck function, and the rates of energy absorption can also be calculated using eq 1. This is exemplified in Figure 5, which shows the computed infrared absorption spectrum of $H^+(NH_3)_n$, $n = 5$, superimposed over the 300 K blackbody function. The dotted line representing the cumulative absorbed power shows very clearly, that while in each case the most intense infrared bands are the OH or NH stretching vibrations, these contribute little to the overall energy absorption from the blackbody background. This is dominated by the weaker, but lower frequency modes between ≈200−1200 cm^{-1}, which overlap more effectively the Planck function.

By comparing the results given in Tables 2 and 3, one can also note that the overall rate of energy absorption of 22.6 kW/mol computed for the water cluster $H^+(H_2O)_4$, is indeed about a factor of 2 larger than that of the corresponding $n = 4$ ammonia cluster, 11.7 kW/mol, and a similar ratio and stronger

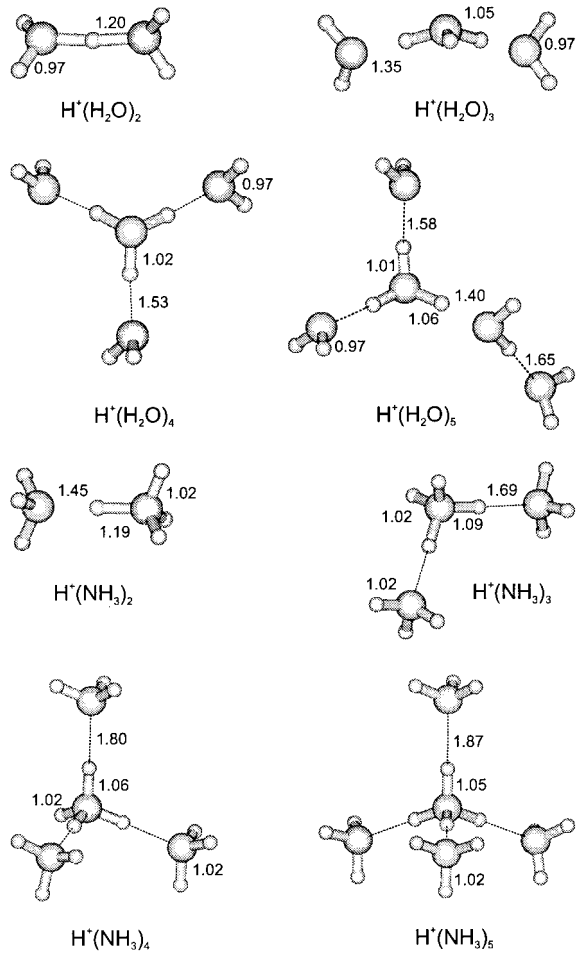

Figure 4. Optimized structures of $H^+(H_2O)_n$, $n = 2-5$, and $H^+(NH_3)_n$, $n = 2-5$. Characteristic distances are indicated in angstroms.

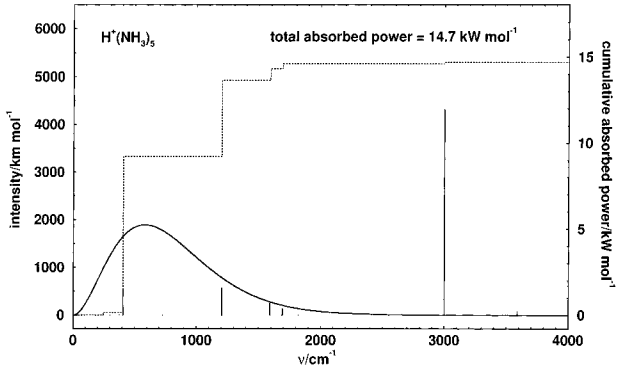

Figure 5. Calculated IR spectrum of $H^+(NH_3)_5$ superimposed over the 300 K Planck distribution function. Intensities for vibrations within 3 cm^{-1} were summed into one peak. The dotted line represents the cumulative absorbed power in kW/mol.

binding of the water ligands is found also for $n = 5$. This confirms that, as outlined above, the higher rates of energy absorption by clusters solvated by water almost perfectly compensate their higher binding energies. This then leads to the observed, very similar fragmentation behavior, and similar slopes of the diagrams like Figures 2 and 3, where the rates k_n are plotted against the number of ligands n, regardless of whether the solvent is water or ammonia. The computation of the rate of energy absorption exemplified in Tables 2 and 3 also confirms the expected, previously discussed approximately linear increase in the energy absorption rates with the number of ligands. It may also be noted that the computed absolute rates of the energy

TABLE 2: Experimental and Calculated Binding Energies for $H^+(H_2O)_n$, $n = 1-5$, Together with the Calculated Average Internal Energy at 300 K and the Total Absorbed power from 298 K Blackbody Radiation

$H^+(H_2O)_n$	$\Delta H^0_{n-1,n}$ exptl [kJ/mol]	$\Delta H^0_{n-1,n}$ calcd [kJ/mol]	average internal energy [kJ/mol]	total absorbed power [kW/mol]
$n = 1$	-691.0[a]	-680.4	0.2	9.6
$n = 2$	-150.6[b]	-148.4	5.0	38.7
$n = 3$	-93.3[b]	-88.3	12.4	20.3
$n = 4$	-71.1[b]	-70.8	20.7	22.6
$n = 5$	-64.0[b]	-49.6	28.9	26.8

[a] Reference 36. [b] Kebarle, P.; Searles, S. K.; Zolla, A.; Scarborough, J.; Arshadi, M. *J. Am. Chem. Soc.* **1967**, *89*, 6393.

TABLE 3: Experimental and Calculated Binding Energies for $H^+(NH_3)_n$, $n = 1-5$, Together with the Calculated Average Internal Energy at 300 K and the Total Absorbed Power from 298 K Black Body Radiation

$H^+(NH_3)_n$	$\Delta H^0_{n-1,n}$ exptl [kJ/mol]	$\Delta H^0_{n-1,n}$ calcd [kJ/mol]	average internal energy [kJ/mol]	total absorbed power [kW/mol]
$n = 1$	-853.6[a]	-843.0	0.1	2.0
$n = 2$	-106.3[b]	-113.2	5.7	34.5
$n = 3$	-72.4[b]	-68.7	13.6	9.1
$n = 4$	-59.4[b]	-55.3	23.5	11.7
$n = 5$	-49.4[b]	-44.0	33.9	14.7

[a] Reference 36. [b] Arshadi, M.; Futrell, J. J. *J. Phys. Chem.* **1974**, *78*, 1482.

TABLE 4: $\Delta H^0_{n-1,n}$ in kJ/mol for the Gas Phase Hydration of H^+ and Ag^+: $X^+(H_2O)_{n-1} + H_2O \rightarrow X^+(H_2O)_n$ (X = Ag, H)

	$n = 1$	$n = 2$	$n = 3$	$n = 4$	$n = 5$
X = H[a]		-150.6	-93.3	-71.1	-64.0
X = Ag[b]	-139.3	-106.3	-62.8	-62.3	-57.3

[a] Kebarle, P.; Searles, S. K.; Zolla, A.; Scarborough, J.; Arshadi, M. *J. Am. Chem. Soc.* **1967**, *89*, 6393. [b] Holland, P. M.; Castleman, A. W., Jr. *J. Chem. Phys.* **1982**, *76*, 4195.

absorption, when compared with the ligand binding enthalpies, are consistent with the measured fragmentation rates, and with the observation that small clusters, e.g., $H^+(H_2O)_5$, fragment on a time scale of many seconds.

Theoretical Investigation of Observed Final Products. In addition to the slope k_f, the fits of the fragmentation behavior are also characterized by a second constant, the intercept n_0. This constant, that is the observation that the fit does not go through the origin is physically simply a reflection of the fact, that the smallest clusters do not fragment at all under the conditions of our experiment. This is due to two important effects. In the first place, while, as already explained above, the larger clusters are quite cold, and their "blackbody" infrared emission can be neglected, this is no longer true for the smallest, more stable clusters. The ligands closer to the ionic core of the cluster are more strongly bound than those at the periphery or "surface" of the larger clusters. Their evaporation requires more energy (see Tables 4 and 5), and the cluster temperature has to rise higher before a ligand can evaporate. Eventually, the smallest clusters will reach thermal equilibrium with the apparatus walls, and at this point the rate of energy absorption will be equivalent to the rate of their infrared emission, and the cluster heating will essentially stop.

Inspection of some of the final products, for instance of the hydrated silver cation clusters shows, however, that this cannot

TABLE 5: $\Delta H^0_{n-1,n}$ in kJ/mol for the Gas Phase Association of NH_3 to H^+ and Ag^+: $X^+(NH_3)_{n-1} + NH_3 \rightarrow X^+(NH_3)_n$ (X = Ag, H)

	$n=1$	$n=2$	$n=3$	$n=4$	$n=5$
X = H[a]		−106.3	−72.4	−59.4	−49.4
X = Ag	−203.8[c]	−154.4[b]	−61.1[b]	−54.4[b]	−53.6[b]

[a] Arshadi, M.; Futrell, J. J. *J. Phys. Chem.* **1974**, *78*, 1482. [b] Holland, P. M.; Castleman, A. W., Jr. *J. Chem. Phys.* **1982**, *76*, 4195. [c] Deng, H.; Kebarle, P. *J. Phys. Chem. A* **1998**, *102*, 571.

be the only explanation, and that some other effects must contribute to the small ion stability. As can be seen in Figure 1 and Figure 2a, while $Ag^+(H_2O)_4$ fragments with a nonnegligible rate constant ($k = 0.13 \pm 0.02$ s^{-1}) the next smaller cluster, $Ag^+(H_2O)_3$ does not fragment at all on the time scale of our experiment. Their binding energies which are given in Table 4 differ by only 0.5 kJ/mol, and this small difference cannot provide an adequate reason for the observed large difference in the fragmentation rates.

The explanation for this effect can, however be found by examining Tables 2 and 3. These show, besides the experimental and computed binding energies and the rates of the infrared energy absorption, also the average internal energies of the clusters when they reach equilibrium with the apparatus wall, that is at a temperature of approximately 300 K. One can easily see in these tables, that even at room temperature, the energy content of the smallest clusters is very small. This is due not only to the smaller number of degrees of freedom, but more importantly to their relatively rigid structures, and to the absence of low-frequency vibrational modes. As the clusters grow, and additional, weaker bound ligands are added to the second or third solvation shell, the number of low-frequency modes increases, and the amount of internal energy at 300 K grows drastically. Thus, the internal energy of a proton solvated by two or three water molecules is ≈5.0 and 12.4 kJ/mol, respectively, with the corresponding values for two or three ammonia ligands being only slightly larger, 5.7 and 13.6 kJ/mol (see Tables 2 and 3). These values are small compared with the respective binding energies, so that even at 300 K the energetic threshold for ligand loss is very unlikely to be reached. On the other hand, for $n = 5$ the computed internal energies are 28.9 kJ/mol for water and 33.9 kJ/mol for ammonia clusters, which is already comparable with the binding energies. Thus, in the above-mentioned example of solvated $Ag^+(H_2O)_n$ clusters, the reason for the fragmentation of the $n = 4$ cluster, and lack of it for $n = 3$ is the much larger energy content of the larger ion, rather than the small difference in the binding energies. While we have not carried out similar calculations for ammonia solvated Ag^+ clusters, for the protons solvated by ammonia the computed internal energies at 300 K are 13.6 kJ/mol for $n = 3$, and 23.5 kJ/mol for $n = 4$, a difference of nearly 50%, which can easily explain the different fragmentation behavior.

Although it is still difficult to carry out ab initio computations on larger solvated clusters, it is not difficult to estimate their spectra and the distribution of their vibrational modes. These change systematically with cluster size, and using such estimated spectra one can easily compute the approximate energy content of larger clusters. We have carried out such computations of the internal energy as a function of the temperature up to $n \approx 100$. As an example, for a hydrated cluster with $n = 55$, one predicts at room temperature a value of over 400 kJ/mol. At 150 K, a temperature value we have estimated by extrapolation of bulk water properties for clusters in this size range observed in our experiment,[9] the average computed internal energy is 140 kJ/mol, a value which still exceeds by more than a factor of 3 the vaporization enthalpy of water. This just confirms what we stated earlier: the larger clusters can be "metastable", and survive quite long—on the order of the millisecond to second time scale of our experiment—even though they have energies quite high above the threshold for fragmentation. In fact the computations indicate that water clusters in this range (near $n = 55$) would have to be cooled to <70K and ammonia species to <40 K to lower their internal energies below the solvent molar vaporization enthalpy.

It would of course be highly desirable to construct a model based on RRK or RRKM theory that produces both the overall linear dependence of k_n on n as well as the insensitivity of the observed fragmentation rate on the identity of the core ion and the solvating molecule. Upon closer inspection of this idea, serious problems become apparent: An RRK based model would produce unrealistic results due to the assumption that all oscillators have the same frequency. In the larger clusters, the internal energy is mainly stored in the low-frequency modes well below 100 cm^{-1}, while the dissociative mode lies at approximately 250 cm^{-1}. Assuming the 250 cm^{-1} for all oscillators would produce at, for example, 100 K an internal energy that is too low by an order of magnitude. Taking a low-frequency mode, however, would make the fragmentation too facile, since an unrealistically low amount of energy would be required. A model that would be truly superior to the semiquantitative arguments presented here requires extensive numeric modeling based on RRKM theory and the calculated energy absorption rates. This goes well beyond the scope of the present work.

Deviation of Fragmentation Rate from Linearity: Magic Clusters. A closer examination of Figures 2 and 3 indicates that while in general the linear relationship between the fragmentation rates and n is reasonably well obeyed, and in some regions the rate constants indeed follow the linear regression fit quite closely, in others considerable fluctuations can be seen, with the deviations of some specific clusters from the predicted behavior being well outside the error of the experiment. A dramatic example of this behavior are the previously discussed hydrated protons, and the anomalously high stability of the $n = 55$ cluster, with conversely a drastically increased fragmentation rate of the $H^+(H_2O)_{56}$ cluster ion (see Figure 3a). Similarly, Figure 2a shows for hydrated Ag^+ that, for example, the $n = 4-18$ and $n = 33-38$ follow well the fit, but in the region between $n = 41-43$, significant deviations can be seen. Also for hydrated Mg^+ and Al^+ cations such regions where significant deviations occur have been observed. For example for $Al^+(H_2O)_n$ such regions were found between $n = 23-27$ and $n = 36-39$ and for $Mg^+(H_2O)_n$ between $n = 38-41$.[11,12] There has been a considerable amount of discussion[12] of whether solvated clusters of this type should be viewed as more or less rigid, "solid" structures, or as liquidlike, fluxional species. We have argued that the large local deviations from the overall linear behavior (e.g., $n = 55$) suggest the former is closer to the truth, since in fluxional, liquid structures, many structural "isomers" would be present, averaging out any effects of local structure. Perhaps one can conversely argue that in those regions where the deviations from the predicted linear behavior are small, structures are ill-defined, and many isomers are present.

Conclusion

We have investigated ionic clusters solvated by ammonia, and show that similar to hydrated clusters, they are in the collision-free environment of an ICR cell efficiently fragmented by ambient blackbody infrared radiation. Specifically, we have examined the fragmentation of size-selected ionized ammonia

clusters $Ag^+(NH_3)_n$, $n = 4-21$, and $H^+(NH_3)_n$, $n = 5-30$, and compared the results to the corresponding hydrated ions, $Ag^+(H_2O)_n$, $n = 4-45$, as well as to the previously investigated protonated water clusters, $H^+(H_2O)_n$, $n = 5-65$. In all these cases, as well as in the case of several other hydrated cations and anions previously studied, the fragmentation rate constant is linearly dependent on the cluster size n. Slope values obtained by fitting the observed fragmentation rates to the expression $k_n = k_f(n - n_0)$ are found to be essentially identical with $k_f \approx 0.18\ s^{-1}$ not only for all of the hydrated ions studied but also for ions solvated by ammonia. While the equal values of the k_f constant for all hydrates studied reflect the relative insensitivity of the large ligated clusters to the specific nature and polarity of the central ion, the similarity with ions solvated by ammonia is fortuitous, due to accidental cancellation of the effect of the weakened binding in the latter clusters by the less efficient absorption of the blackbody IR radiation.

Acknowledgment. Financial support by the Deutsche Forschungsgemeinschaft, the Fond der Chemischen Industrie and the Leonhard-Lorenz-Stiftung (M.K.B.) is gratefully acknowledged.

Supporting Information Available: Z-matrixes of optimized structures and calculated IR spectra of water and ammonia cations. This material is available free of charge via the Internet at http://pubs.acs.org.

References and Notes

(1) Ng, C.-Y., Baer, T., Powis, I., Eds. *Cluster Ions*; Wiley: New York, 1993.

(2) Haberland, H., Ed. *Clusters of Atoms and Molecules*; Springer: Berlin, 1994; Vol. 2.

(3) Thölmann, D.; Tonner, D. S.; McMahon, T. B. *J. Phys. Chem.* **1994**, *98*, 2002.

(4) Thölmann, D.; Tonner, D. S.; McMahon, T. B. *Chem. Phys. Lett.* **1995**, *233*, 324.

(5) Dunbar, R. C.; McMahon, T. B. *Science* **1998**, *279*, 194.

(6) Rodriguez-Cruz, S. E.; Jockusch, R. A.; Williams, E. R. *J. Am. Chem. Soc.* **1998**, *120*, 5842.

(7) Rodriguez-Cruz, S. E.; Jockusch, R. A.; Williams, E. R. *J. Am. Chem. Soc.* **1999**, *121*, 1986.

(8) Rodriguez-Cruz, S. E.; Jockusch, R. A.; Williams, E. R. *J. Am. Chem. Soc.* **1999**, *121*, 8898.

(9) Schindler, T.; Berg, C.; Niedner-Schatteburg, G.; Bondybey, V. E. *Chem. Phys. Lett.* **1996**, *250*, 301.

(10) Bondybey, V. E.; Schindler, T.; Berg, C.; Beyer, M.; Achatz, U.; Joos, S.; Niedner-Schatteburg, G. In *Recent Theoretical and Experimental Advances in Hydrogen-Bonded Clusters*, Xantheas, S. S., Ed.; NATO ASI Series C; Kluwer: Dordrecht, 2000; Vol. 561.

(11) Berg, C.; Beyer, M.; Achatz, U.; Joos, S.; Niedner-Schatteburg, G.; Bondybey, V. E. *Chem. Phys.* **1998**, *239*, 379.

(12) Beyer, M.; Achatz, U.; Berg, C.; Joos, S.; Niedner-Schatteburg, G.; Bondybey, V. E. *J. Phys. Chem. A* **1999**, *103*, 671.

(13) Achatz, U.; Joos, S.; Berg, C.; Beyer, M.; Niedner-Schatteburg, G.; Bondybey, V. E. *Chem. Phys. Lett.* **1998**, *291*, 459.

(14) Achatz, U.; Joos, S.; Berg, C.; Schindler, T.; Beyer, M.; Albert, G.; Niedner-Schatteburg, G.; Bondybey, V. E. *J. Am. Chem. Soc.* **1998**, *120*, 1876.

(15) Fox, B. S.; Beyer, M. K.; Achatz, U.; Joos, S.; Niedner-Schatteburg, G.; Bondybey, V. E. *J. Phys. Chem. A* **2000**, *104*, 1147.

(16) Schindler, T.; Berg, C.; Niedner-Schatteburg, G.; Bondybey, V. E. *Chem. Phys. Lett.* **1994**, *229*, 57.

(17) Berg, C.; Achatz, U.; Beyer, M.; Joos, S.; Albert, G.; Schindler, T.; Niedner-Schatteburg, G.; Bondybey, V. E. *Int. J. Mass Spectrom. Ion Process* **1997**, *167/168*, 723.

(18) Bondybey, V. E.; Beyer, M.; Achatz, U.; Joos, S.; Niedner-Schatteburg, G.; *Isr. J. Chem.* **1999**, *39*, 213.

(19) Fraser, G. T.; Nelson, D. D., Jr.; Gerfen, G. J.; Klemperer, W. *J. Chem. Phys.* **1985**, *82*, 2535.

(20) Curtiss, L. A.; Pople, J. A. *J. Mol. Spectrosc.* **1975**, *55*, 1.

(21) Curtiss, L. A.; D. J. Frurip, D. J.; Blander, M. *Chem. Phys. Lett.* **1978**, *54*, 575.

(22) Curtiss, L. A.; D. J. Frurip, D. J.; Blander, M. *J. Chem. Phys.* **1979**, *71*, 2703.

(23) (a) Ichihashi, M.; Yamabe, J.; Murai, K.; Nonose, S.; Hirao, K.; Kondow, T. *J. Phys. Chem.* **1996**, *100*, 10050. (b) Park, J. K. *J. Phys. Chem. A* **2000**, *104*, 5093.

(24) Bérces, A.; Nukada, T.; Margl, P.; Ziegler, T. *J. Phys. Chem. A* **1999**, *103*, 9693.

(25) Berg, C.; Schindler, T.; Niedner-Schatteburg, G.; Bondybey, V. E. *J. Chem. Phys.* **1995**, *102*, 4870.

(26) Beyer, M.; Berg, C.; Görlitzer, H.; Schindler, T.; Achatz, U.; Albert, G.; Niedner-Schatteburg, G.; Bondybey, V. E. *J. Am. Chem. Soc.* **1996**, *118*, 7386.

(27) Frisch, M. J.; Trucks, G. W.; Schlegel, H. B.; Scuseria, G. E.; Robb, M. A.; Cheeseman, J. R.; Zakrzewski, V. G.; Montgomery, J. A., Jr.; Stratmann, R. E.; Burant, J. C.; Dapprich, S.; Millam, J. M.; Daniels, A. D.; Kudin, K. N.; Strain, M. C.; Farkas, O.; Tomasi, J.; Barone, V.; Cossi, M.; Cammi, R.; Mennucci, B.; Pomelli, C.; Adamo, C.; Clifford, S.; Ochterski, J.; Petersson, G. A.; Ayala, P. Y.; Cui, Q.; Morokuma, K.; Malick, D. K.; Rabuck, A. D.; Raghavachari, K.; Foresman, J. B.; Cioslowski, J.; Ortiz, J. V.; Baboul, A. G.; Stefanov, B. B.; Liu, G.; Liashenko, A.; Piskorz, P.; Komaromi, I.; Gomperts, R.; Martin, R. L.; Fox, D. J.; Keith, T.; Al-Laham, M. A.; Peng, C. Y.; Nanayakkara, A.; Gonzalez, C.; Challacombe, M.; Gill, P. M. W.; Johnson, B.; Chen, W.; Wong, M. W.; Andres, J. L.; Gonzalez, C.; Head-Gordon, M.; Replogle, E. S.; Pople, J. A. *Gaussian 98*, Revision A.7; Gaussian, Inc.: Pittsburgh, PA, 1998.

(28) Becke, A. D. *Phys. Rev. A* **1988**, *38*, 3098.

(29) Becke, A. D. *J. Chem. Phys.* **1993**, *98*, 1372.

(30) Becke, A. D. *J. Chem. Phys.* **1993**, *98*, 5648.

(31) Lee, C.; Yang, W.; Parr, R. G. *Phys. Rev. B* **1988**, *37*, 785.

(32) Lee, E. P. F.; Dyke, J. M. *Mol. Phys.* **1991**, *73*, 375.

(33) (a) Corongiu, G.; Kelterbaum, R.; Kochanski, E. *J. Phys. Chem.* **1995**, *99*, 8038. (b) Kelterbaum, R.; Kochanski, E. *J. Chem. Phys.* **1995**, *99*, 12493.

(34) Wei, D. Q.; Salahub, D. R. *J. Chem. Phys.* **1997**, *106*, 6086.

(35) Beyer, M.; Savchenko, E. V.; Niedner-Schatteburg, G.; Bondybey, V. E. *Low Temp. Phys.* **1999**, *25*, 814.

(36) Mallard, W. G., Linstrom, P. J., Eds.; *NIST Chemistry WebBook*; NIST Standard Reference Database Number 69; National Institute of Standards and Technology: Gaithersburg, MD 20899, February 2000. (http://webbook.nist.gov.)

(37) Lide, D. R., Ed. In *Chemical Rubber Company Handbook of Chemistry and Physics*, 77th ed.; CRC Press: Boca Raton, FL, 1996.

(38) Barnett, R. N.; Landman, U. *J. Phys. Chem. A* **1997**, *101*, 164.

(39) Barnett, R. N.; Landman, U. *J. Phys. Chem.* **1995**, *99*, 17305.

(40) Ng, C. Y.; Trevor, D. J.; Tiedemann, P. W.; Ceyer, S. T.; Kronebusch, P. L.; Mahan, B. H.; Lee, Y. T. *J. Chem. Phys.* **1977**, *67*, 4235.

(41) Tomoda, S.; Kimura, K. *Chem. Phys.* **1983**, *82*, 215.